Measurement of Nucleotide Release Kinetics in Single Skeletal Muscle Myofibrils during Isometric and Isovelocity Contractions using Fluorescence Microscopy

Shigeru Chaen,* Ibuki Shirakawa,* Clive R. Bagshaw,# and Haruo Sugi*
*Department of Physiology, School of Medicine, Teikyo University, Tokyo 173, Japan, and #Department of Biochemistry, University of Leicester, Leicester LE1 7RH, U.K.

ABSTRACT Rabbit psoas muscle myofibrils, in the presence of the fluorescent nucleotide analog 2′(3′)-O-[N-[2-[[Cy3]amido]ethyl]carbamoyl]-adenosine 5′ triphosphate (Cy3-EDA-ATP), showed selective fluorescence staining of the A-band with a reduced fluorescence at the M-line. Addition of Cy3-EDA-ATP to a myofibril in the presence of Ca^{2+} caused auxotonic shortening against a compliant glass microneedle. These results indicate that Cy3-EDA-ATP is a substrate for myosin in the myofibril system. The kinetics of nucleotide release from a single myofibril, held isometrically between two needles, were measured by the displacement of prebound Cy3-EDA-ATP on flash photolysis of caged ATP. The A-band fluorescence of the myofibril decayed exponentially with a rate constant of 0.3 s^{-1} at 8°C, an order of magnitude faster than that for isolated thick filaments in the absence of actin. When a myofibril was imposed to shorten with a constant velocity by a piezoelectric actuator, the nucleotide displacement rate constant initially increased to 0.7 s^{-1} with increasing shortening velocity and then declined with a further increase in shortening velocity. These results demonstrate that the displacement rates of Cy3-EDA-nucleotides bound to the cross-bridges in the contracting myofibril reflect a process that shows strain dependence.

INTRODUCTION

Solving the question about how muscle modulates its energy output depending on the load has been regarded as one of the crucial aspects of understanding the mechanism of muscle contraction. When stimulated muscle is allowed to shorten against a load, the total energy liberation (heat + work) is increased compared to that under isometric condition (the Fenn effect: Fenn, 1923, 1924). Hill (1964) found that the rate of total energy liberation was at maximum at 0.5 V_{max} and declined with increasing shortening velocity. The rate of ATP splitting was also shown to be at maximum at this velocity (Kushmerick and Davies, 1969). Subsequently, the rate of ATP hydrolysis during shortening at V_{max} was reported to be lower than that for the enthalpy liberation (Rall et al., 1976; Homsher et al., 1981; Ohno and Kodama, 1991). To interpret the Fenn effect, A. F. Huxley (1957) has postulated that cross-bridge detachment is relatively slow in active isometric muscle, but in actively shortening muscle, the resulting low or negative mechanical strain of the cross-bridge markedly accelerates the detachment rate. The lower rate of ATP hydrolysis during rapid shortening has been explained by cross-bridges detaching before releasing their hydrolysis products (Huxley, 1973; Rall et al., 1976; Homsher, 1987; Bagshaw, 1993; Cooke et al., 1994).

A number of the states involved in the cyclic interaction of actomyosin have been identified by using isolated muscle proteins in solution and skinned muscle fibers (for reviews see Taylor, 1979; Cooke, 1986; Hibberd and Trentham, 1986; Goldman, 1987). Kinetic studies using isolated proteins, however, are insufficient to interpret the detailed characteristics of muscle contraction (for reviews see Sugi, 1992, 1997), especially with regard to work production using the chemical energy of ATP hydrolysis, because actin-myosin interaction in solution takes place under unloaded conditions.

The purpose of the present study is to measure actomyosin ATPase kinetics under various loads. Here we have devised a method for measuring directly how the rate of ATP turnover depends on the mechanical condition of the cross-bridges. This rate was estimated from the displacement of fluorescent nucleotides bound to cross-bridges by flash photolysis of caged ATP (Conibear and Bagshaw, 1996). In this study, we used a single myofibril that is amenable to both rapid kinetic and mechanical measurements (Ma and Taylor, 1994; Herrmann et al., 1993, 1994; Friedman and Goldman, 1996; Bartoo et al., 1993; Colomo et al., 1995; Lionne et al., 1995, 1996). A single myofibril was attached to a pair of glass needles by the method of Anazawa et al. (1992), so that various mechanical conditions could be applied to the myofibril. The fluorescent image of the myofibril was observed under a microscope, with a laser scanning attachment for confocal microscopy. The latter was found to be indispensable for reducing the background fluorescence from the bulk solution containing fluorescent nucleotides at >1 μM concentrations.

It was shown that the observed nucleotide displacement rate depended on the shortening velocity, reaching a maxi-

Received for publication 24 February 1997 and in final form 26 June 1997.
Address reprint requests to Dr. Shigeru Chaen, Department of Physiology, School of Medicine, Teikyo University, Kaga 2-11-1, Itabashi-ku, Tokyo 173, Japan. Tel.: 81-3-3964-1211, ext. 2155; Fax: 81-3-5375-8789; E-mail: chaen@med.teikyo-u.ac.jp.

0006-3495/97/10/2033/10 $2.00

mum at ~50% of the observed V_{max} for sliding. Thus measurements of nucleotide exchange kinetics using fluorescent nucleotide and flash photolysis of caged ATP are useful in studying the coupling between the ATPase rate and work in contracting muscle myofibrils. A preliminary report of related work has been presented (Chaen et al., 1996).

MATERIALS AND METHODS

Solutions

The Ca^{2+}-free rigor solution contained 60 mM *N,N*-bis(2-hydroxyethyl)-2-aminoethanesulfonic acid (BES) (pH 7.1), 53 mM EGTA, 3.2 mM $MgCl_2$, 30 mM dithiothreitol (DTT), and 1% β-mercaptoethanol. The Ca^{2+}-rigor solution contained 60 mM BES (pH 7.1), 33 mM 1,6-diaminohexane-*N,N,N′,N′*-tetraacetic acid (HDTA), 20 mM EGTA, 20 mM $CaCl_2$, 1.3 mM $MgCl_2$, 30 mM DTT, and 1% β-mercaptoethanol. Unless otherwise stated, the activating solution contained Ca^{2+}-rigor solution, plus 10 μM Cy3-EDA-ATP, 5.2 mM caged ATP (Calbiochem, San Diego, CA), and the ATP-regenerating reagents 20 mM phosphocreatine (Sigma, St. Louis, MO) and 150 units/ml creatine phosphokinase (Sigma). The free Ca^{2+} concentration in the activating solution was calculated to be ~30 μM. Although EDA derivatives of ATP are poor substrates for creatine kinase, the back-up system helps to maintain the concentration of ATP after flash photolysis.

Cy3-EDA-ATP (Fig. 2 *C*) was synthesized by reacting Cy3.29-OSu succinimidyl ester (Mujumdar et al., 1993) with 2′(3′)-*O*-[*N*-(2-aminoethyl)carbamoyl]-adenosine-5′-triphosphate (EDA-ATP) (Saito et al., 1995; Eccleston et al., 1996; Oiwa et al., 1996; Conibear et al., 1996). Cy3-EDA-ADP was prepared by reacting Cy3.29-OSu succinimidyl ester with EDA-ADP. EDA-ATP and EDA-ADP were synthesized by the method of Cremo et al. (1990). Fractions of Cy3-EDA-ATP (or Cy3-EDA-ADP) were collected from a SAX column (Synchropak Q300A; MICRA Scientific, Lafayette, IN), using a Hitachi high-performance liquid chromatography (HPLC) system (L-6200, L-4200, and D-2500; Hitachi, Tokyo, Japan) and elution with 0.6 M ammonium dihydrogen phosphate at pH 4.0 plus 20% methanol. The pooled fractions were diluted with distilled water, salt was removed using DE52 cellulose and 0.5 M triethylamine bicarbonate (TEAB), and the residual TEAB was removed by repeated evaporation with methanol. No contamination of Cy3.29-OSu and EDA-ATP (or EDA-ADP) in the final product was found by HPLC analysis. The concentration of Cy3-EDA-ATP or Cy3-EDA-ADP was determined assuming an absorbance coefficient A_{550} of 150,000 M^{-1} cm^{-1}. Cy3.29-OSu succinimidyl ester was purchased from Amersham Life Science (Pittsburgh, PA). BES, EGTA, and HDTA were from Dojindo Laboratories (Kumamoto, Japan). Other chemicals were of analytical grade.

Preparations of myofibrils

Bundles of muscle fibers (~3 mm in diameter) were dissected from rabbit psoas muscle and tied to glass rods, kept in a 50% glycerol solution containing 5 mM potassium phosphate (pH 6.8) and 2 mM EGTA at 0°C overnight, then stored at −20°C after the solution was changed. Myofibrils were prepared by a similar procedure of Anazawa et al. (1992): small strips of muscle fibers (~0.5 mm in diameter and ~10 mm in length) were dissected from the glycerinated psoas muscle fibers, put into the Ca^{2+}-free rigor solution of 5 ml in a test tube, and homogenized with a homogenizer (Polytron, Type PT10/35; Kinematica, Littau/Lucerne, Switzerland) for 1 min at a moderate speed of rotation. Myofibrils were then kept in the Ca^{2+}-free rigor solution at 0°C and used on the same day. Myofibrils prepared in this manner had a sarcomere length of ~2.5 μm. In some cases, a myofibril attached to glass needles was prestretched to between 3.2 and 3.4 μm sarcomere length in relaxing solution containing 1 mM ATP and then returned to the Ca^{2+}-free rigor solution.

Experimental setup

Fig. 1 shows a schematic diagram of the apparatus for measuring the displacement of fluorescent nucleotides in the contracting myofibrils by the flash photolysis of caged ATP. A single myofibril was held horizontally in an experimental trough with a pair of glass microneedles by the method of Anazawa et al. (1992). Each end of the myfibril was attached to a glass needle, which, in turn, was connected to water-pressure-controlled 3-D micromanipulators (WR-90; Narishige, Tokyo, Japan) to manipulate the myofibril under the microscope. For experiments involving myofibril shortening, one glass microneedle was used as a fixed end, and the other end was attached to a piezoelectric actuator (PSt150/7/90; Dr. Lutz Pickelmann Piezomechanik Optik, Munich, Germany). The piezoelectric actuator was driven by a piezo drive amplifier (M-2617; MES-TEK, Wako, Japan) and function generator/arbitrary wave form generator (HP33120A; Hewlett-Packard, Loveland, CO) to impose constant-velocity shortening on the myofibril preparation. In the case of isometric contractions, the piezo drive amplifier was turned off. We used stiff glass microneedles (over 200 pN/nm), except for the experiments allowing auxotonic shortening of the myofibril. The experimental trough (20 × 2.5 × 1 mm) was made of brass with a ~0.2-mm-thick glass window, coupled to the microscope objective lens with immersion oil. After the myofibril was mounted on the needles in the trough, the upper surface of the solution was covered with a coverslip.

The myofibril in a solution containing fluorescent nucleotide was observed with an inverted fluorescent microscope (IMT2; SPlan Apo 100 × oil-immersion objective lens [N.A. 1.4]; Olympus, Tokyo, Japan). To reduce the background fluorescence emitted from the surrounding solution, a laser scanning unit for confocal microscopy (Insight Plus; scanning rate of 120 frames/s; Meridian, Okemos, MI) was installed on the microscope. The excitation source was an argon ion laser (Innova 307; Coherent, Santa Clara, CA). The laser output (514.5 nm, 50 mW) was focused on an optical fiber coupled to the laser scanning unit. Images were recorded with a silicon intensified target (SIT) camera (C2400-08; Hamamatsu Photonics, Hamamatsu, Japan) and an image processor (Argus 10; Hamamatsu Pho-

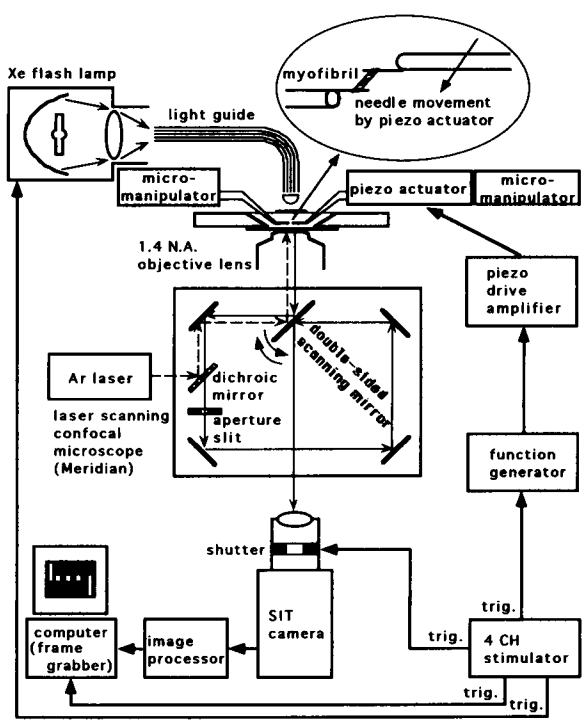

FIGURE 1 Schematic diagram of the apparatus used for measuring the displacement rate of fluorescent-nucleotides in the contracting myofibrils by flash photolysis of caged ATP (see Materials and Methods for details).

tonics), and the successive video frames were stored on a personal computer (Power Macintosh 7600/120; Apple Computer Japan, Tokyo, Japan) through a frame grabber board (LG3 PCI; Scion, Frederick, MD).

Cy3-EDA nucleotides bound to actomyosin in the myofibril were displaced with ATP generated from caged ATP using a xenon flash lamp apparatus (SA-200E; Eagle Shouji, Tokyo, Japan). The light guide from the flash lamp was placed just over the coverslip on the experimental trough. To avoid damage to the SIT camera by the intense flash light, an electronic shutter (EC601; Copal, Tokyo, Japan) was positioned between the microscope and the SIT camera.

Electronic stimulators (SEN-7013 and SEN-3301; Nihon Kohden, Tokyo, Japan), with adjustable time delays and pulse durations, were used to trigger the frame grabber board in the computer, the protective electronic shutter, the flash lamp, and the function generator generator that controlled the muscle shortening speed, in the required sequence.

To regulate the trough temperature, water was circulated into a brass block attached to the trough and another block jacketing the objective. Before the experiment, temperatures were checked by putting a fine thermocoupled needle (Hayashi Denkou, Tokyo, Japan) into the trough. Experiments were performed at 8°C to slow down events of interest to less than 1 s^{-1}.

Experimental procedure and data analysis

Rate constants for fluorescent nucleotides displacement from the myofibril on flash photolysis of caged ATP were calculated by the method of Conibear and Bagshaw (1996). A video image sequence of the region around the fluorescent myofibril was captured using NIH Image (public domain application written by Wayne Rasband, National Institutes of Health) and a dual time base controlled by a customized macro program. From the series of video images, the mean fluorescence intensity of the myofibril was computed as a function of time. The data were then analyzed to determine the displacement rate constant by nonlinear least-squares fitting to an exponential function using Kaleidagraph (Synergy Software, Reading, PA).

In experiments involving myofibril shortening, immediately after the flash photolysis, ramp signals were generated from the function generator to allow the myofibril to shorten at a defined constant velocity. The amount of ramp shortening was set to ~20% of the myofibril length; thereafter the myofibril length was held constant until the myofibril fluorescence diminished to zero. Displacement rates of Cy3-EDA nucleotides in the shortening phase were estimated from the initial part of the fluorescence decay, which corresponded to the ramp shortening.

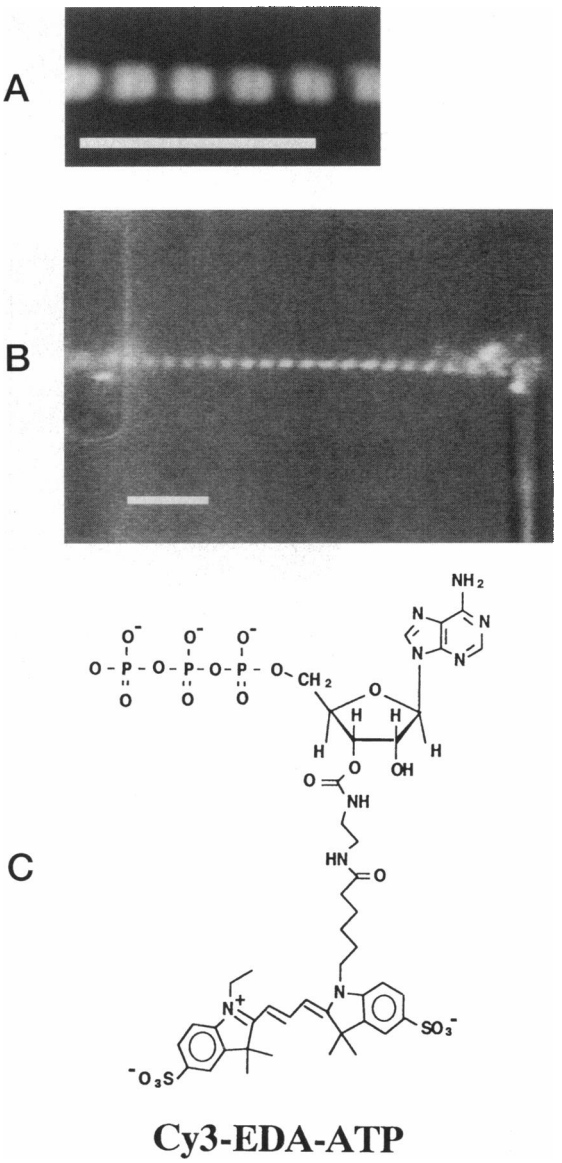

FIGURE 2 Fluorescence images of single rabbit skeletal muscle myofibrils in a solution containing Cy3-EDA-ATP. (*A*) A fluorescence micrograph of a myofibril mounted between two coverslips, taken on Kodak Tri-X 400 35-mm film. The myofibril preparation was bathed in a solution containing the Ca^{2+}-free rigor solution (60 mM BES (pH 7.1), 53 mM EGTA, 3.2 mM $MgCl_2$, 30 mM DTT) and 1 μM Cy3-EDA-ATP. (*B*) Video image of a fluorescent myofibril recorded with a SIT camera. Both ends of the myofibril were held by a pair of glass microneedles, which are seen on the right and left sides. The myofibril preparation was in a solution containing the Ca^{2+}-free rigor solution and 0.2 μM Cy3-EDA-ATP. Scale bars, 10 μm. (*C*) Structure of Cy3-EDA-ATP.

RESULTS

Myofibrils with Cy3-EDA-ATP

A fluorescence micrograph of an isolated rabbit skeletal muscle myofibril is shown in Fig. 2 *A*. Perfusion of the myofibril with the Ca^{2+}-free rigor solution containing 1 μM Cy3-EDA-ATP (Fig. 2 *C*) caused selective fluorescence staining of the A-band, with a reduced fluorescence at the M-line. Fig. 2 *B* shows a video image of a fluorescent myofibril held by glass microneedles. The addition of excess ATP to this myofibril caused disappearance of the A-band fluorescence, suggesting that Cy3-EDA-ATP (probably as its product complex, Cy3-EDA-ADP · P_i; see Discussion) was bound to the myosin active site and was displaced by ATP.

Fig. 3 *A* shows successive video images of auxotonic shortening of myofibril against a compliant microneedle (1 pN/nm). At time 0, a solution containing Ca^{2+}-rigor solution and 5 μM Cy3-EDA-ATP was perfused into the trough. The force developed was calculated by measuring the displacement of the compliant needle on the video image (Fig. 3 *B*, *filled circles*). The auxotonic shortening of a myofibril with 5 μM Cy3-EDA-ATP was found to be comparable to that with 5 μM ATP (Fig. 3 *B*, *open circles*). In these experiments the initial shortening velocity is slow because it is limited by the internal resistance from rigor links (K_m for shortening $\approx$ 150 μM ATP; Cooke and Bialek, 1979).

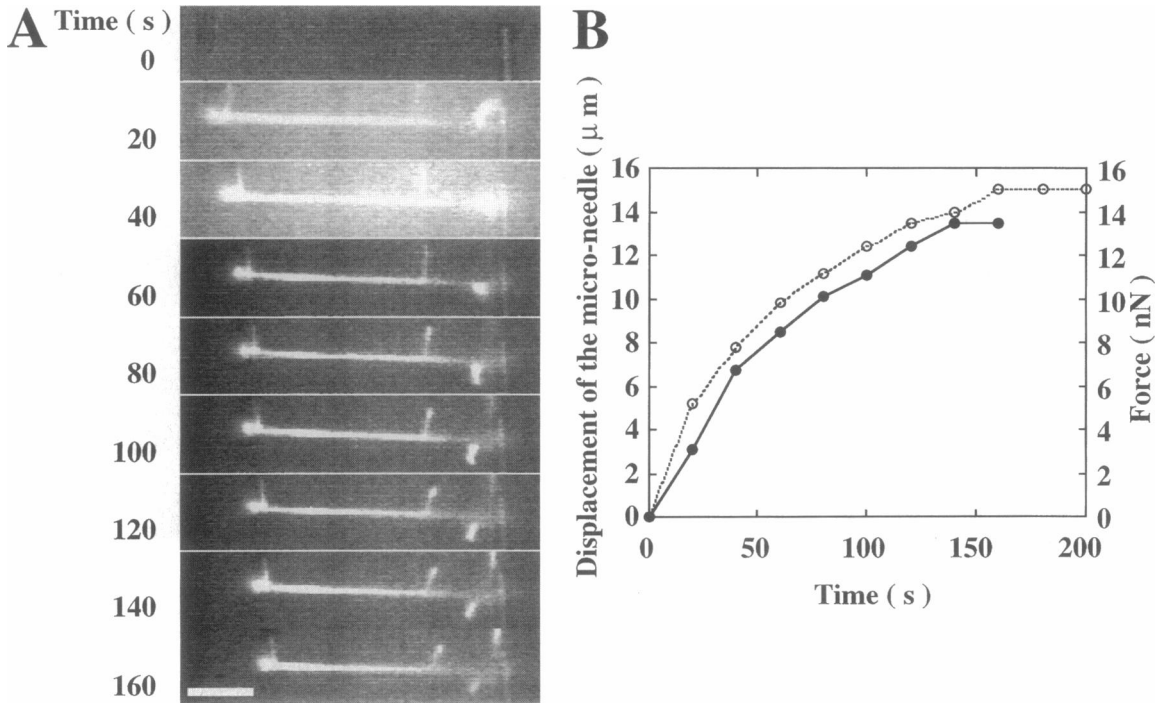

FIGURE 3 Auxotonic shortening of a myofibril against a compliant glass microneedle (1 pN/nm). (*A*) Selected video images of the bending movement of the compliant glass microneedle. A single myofibril was fixed to a pair of glass microneedles (*left microneedle*: 1 pN/nm; *right microneedle*: 200 pN/nm). At time 0, Ca^{2+}-rigor solution (60 mM BES (pH 7.1), 33 mM HDTA, 20 mM EGTA, 20 mM $CaCl_2$, 1.3 mM $MgCl_2$, 30 mM DTT) and 5 μM Cy3-EDA-ATP was perfused into the experimental trough. Scale bar, 10 μm. (*B*) Time course of force development. ●, Data from a myofibril in 5 μM Cy3-EDA-ATP; ○, data from 5 μM ATP instead of 5 μM Cy3-EDA-ATP.

Fig. 4 shows fluorescence intensities of myofibrils (sarcomere length 2.5 μm) as a function of Cy3-EDA-ATP and Cy3-EDA-ADP concentration. The K_m or K_d for nucleotide binding was 2.6 μM for Cy3-EDA-ATP and >30 μM for Cy3-EDA-ADP. The latter was more difficult to characterize because of the weaker binding and hence higher background fluorescence.

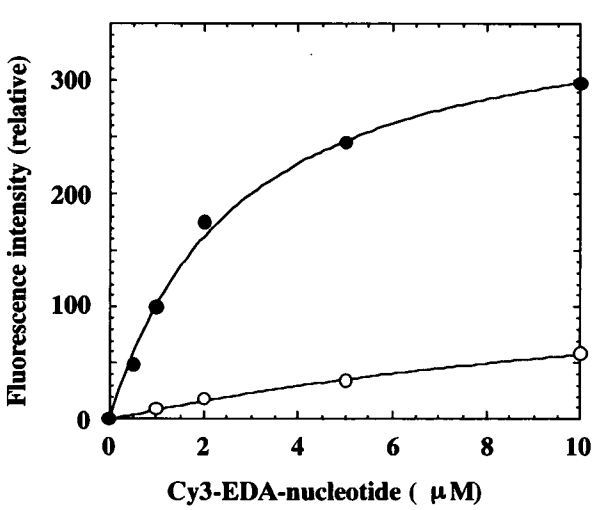

FIGURE 4 Dependence of fluorescence intensity of a myofibril on the concentration of Cy3-EDA-ATP (●) or Cy3-EDA-ADP (○) in the Ca^{2+}-free rigor solution. The myofibril fluorescence intensities were expressed as a relative value of that at 1 μM Cy3-EDA-ATP. The data points were fitted to a hyperbolic curve, which gave a K_m of 2.6 μM for Cy3-EDA-ATP, and a K_d of ~50 μM for Cy3-EDA-ADP.

Displacement of Cy3-EDA nucleotides during isometric contraction

Fig. 5 *A* shows typical successive video images of the displacement of Cy3-EDA nucleotide bound to cross-bridges in the myofibril by flash photolysis of caged ATP during isometric contraction. Fig. 5 *B* shows the exponential decay in Cy3 fluorescence with time. Fig. 5 was from the experiment at 1 μM Cy3-EDA-ATP in the presence of Ca^{2+} with 500 μM caged ATP. The concentration ratio of caged ATP to Cy3-EDA-ATP was set at ~500, because the caged ATP is a weak competitive inhibitor for myosin active site (Thirwell et al., 1995), and hence higher concentrations of caged ATP decreased the fluorescence intensity. With a single xenon flash, ~20% of the caged ATP was photolysed, which was enough to displace the Cy3-EDA nucleotides in the myofibril. Quantitative analysis of the fluorescence decay curve of Fig. 5 *B* yielded a rate constant of 0.56 s^{-1}.

Fig. 6 shows the relation between the displacement rate and the concentration of Cy3-EDA-ATP in the presence and absence of Ca^{2+}. It was noted that the rate in the absence of

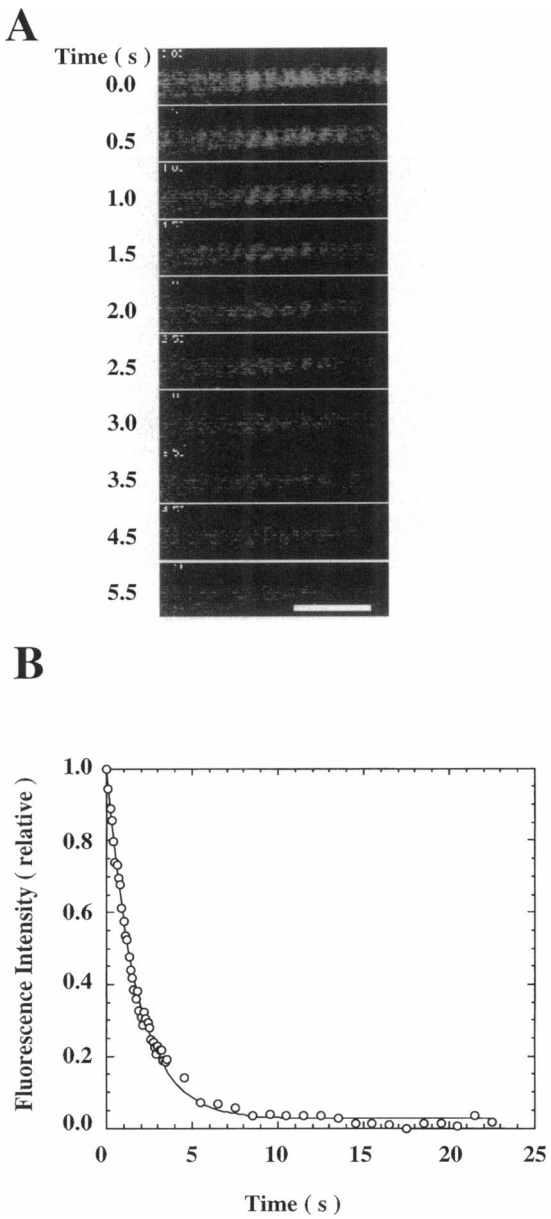

FIGURE 5 Typical experiment showing the displacement of Cy3-EDA nucleotide in the myofibril by flash photolysis of caged ATP under isometric conditions. The solution composition was the same as the activating solution described in Materials and Methods, except for 1 μM Cy3-EDA-ATP and 500 μM caged ATP. (*A*) Selected video images of the fluorescent myofibril, showing the displacement of fluorescent nucleotide bound to the cross-bridge in the myofibril by flash photolysis of caged ATP. Scale bar, 10 μm. (*B*) Quantitative analysis of the displacement of Cy3-EDA nucleotide. The data points were fitted to a single exponential, which gave a rate constant of 0.56 s^{-1}.

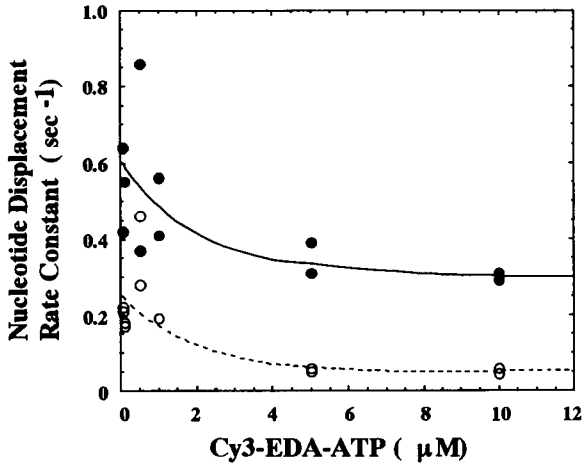

FIGURE 6 Relation between the observed displacement rate constant and the Cy3-EDA-ATP concentration. ●, Rate in the solution containing the Ca^{2+}-rigor solution (30 μM free concentration), and the ATP-regenerating reagents; ○, solution containing the Ca^{2+}-free rigor solution and the ATP-regenerating reagents. The concentrations of caged ATP used were between 0.1 and 5 mM to maintain a concentration ratio of 500 with respect to the Cy3-EDA-ATP concentration (0.2–10 μM). The data shown were obtained from different myofibril preparations. Curves were drawn by eye.

Ca^{2+} was about six times lower than that in the presence of Ca^{2+}. However, because the initial Cy3-EDA-ATP concentration was relatively low, the predominance of rigor cross-bridges is likely to partially override the regulatory mechanism in the absence of Ca^{2+} (Bremel and Weber, 1972). The observed displacement rate constants were more variable and often higher at lower concentrations of Cy3-EDA-ATP, in both the presence and absence of Ca^{2+}. It is possible that at low nucleotide concentrations, the Cy3-EDA-ATP becomes depleted and the Cy3-EDA-ADP concentration builds up locally within the myofibril lattice. To minimize this problem, the concentration of Cy3-EDA-ATP was set at 10 μM to monitor the nucleotide release kinetics during shortening (see below).

The experiments described above were carried out at a sarcomere length of 2.5 μm, and thus the thick filaments were close (80%) to full overlap with the actin filaments. As a control, experiments were performed at a longer sarcomere length (3.3 μm) in the absence of Ca^{2+}. The displacement rate constant for Cy3-EDA-ATP was 0.034 s^{-1} (n = 5; SD = 0.009) at 8°C, lower than the values at 2.5 μm. This value is close to that expected for displacement from the myosin filament alone (Conibear and Bagshaw, 1996; Eccleston et al., 1996; Oiwa et al., 1996).

Attempts were made to follow directly the displacement of Cy3-EDA-ADP. Fig. 7 shows the images of the displacement of Cy3-EDA-ADP prebound to the myofibril by flash photolysis of caged ATP. The image of the fluorescent myofibril before the flash was not clear compared to that in Cy3-EDA-ATP (Fig. 5) because of the lower affinity of Cy3-EDA-ADP for the myofibril, and the displacement rate was too fast to determine accurately. When a myofibril was stretched to 3.4 μm sarcomere length, the image in the presence of Cy3-EDA-ADP was marginally improved and the displacement rate constant was estimated to be 0.42 s^{-1}. This is an order of magnitude faster than that for Cy3-EDA-ATP under comparable conditions.

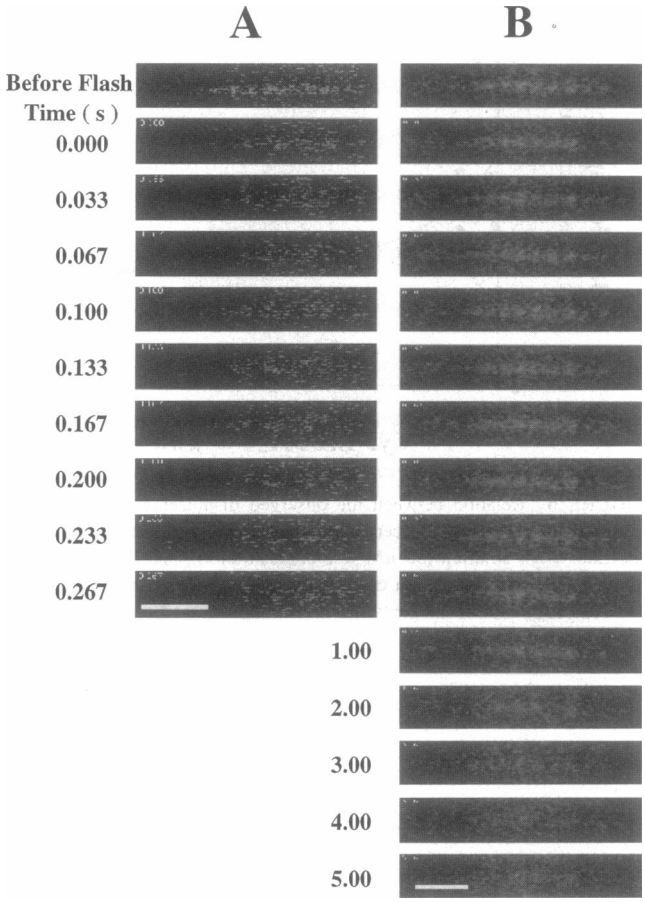

FIGURE 7 Successive video images showing the displacement of Cy3-EDA-ADP from myofibrils (*A*) in the Ca^{2+}-rigor solution at 2.5 μm sarcomere length and (*B*) in the Ca^{2+}-free rigor solution at 3.5 μm sarcomere length, by flash photolysis of caged ATP under isometric conditions. The concentrations of Cy3-EDA-ADP and caged ATP were 14 μM and 280 μM, respectively. Scale bar, 10 μm.

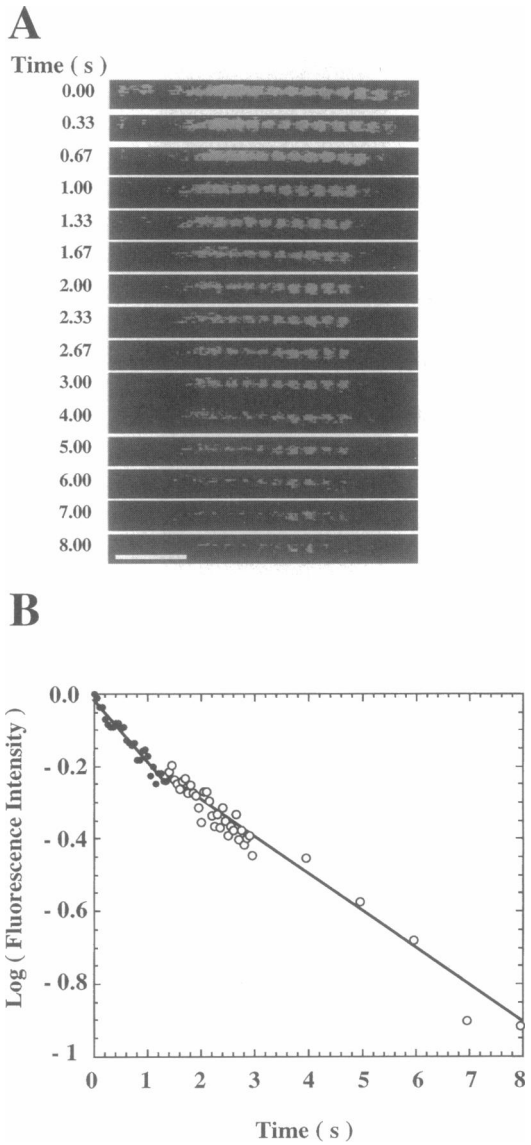

FIGURE 8 Typical experiment showing the displacement of Cy3-EDA nucleotide in the myofibril by flash photolysis of caged ATP during shortening. The myofibril preparation was bathed in activating solution. (*A*) Selected video images of the fluorescent myofibril, showing the displacement of fluorescent nucleotide bound to the cross-bridge in the myofibril by flash photolysis of caged ATP, first during shortening for ~20% myofibril length from time 0 to 1.5 s (0.13 Lo/s), and then held under isometrically. Scale bar, 10 μm. (*B*) Logarithmic plot of the decay of the fluorescence intensities to demonstrate its biphasic nature. Closed and open symbols represent the shortening and isometric phases, respectively. The line represents a linear regression to the data, which gave rate constants of 0.4 s^{-1} and 0.24 s^{-1} for the shortening and isometric phases, respectively.

Displacement of Cy3-EDA nucleotides during isovelocity shortening

To investigate whether the Cy3-EDA-ATP turnover rate is increased during shortening, as seen in intact muscle (Kushmerick and Davies, 1969), the myofibril was imposed to shorten immediately after xenon flash photolysis of caged ATP, and the fluorescence decay from prebound Cy3-EDA nucleotide was measured simultaneously. Fig. 8 *A* shows representative video images of the fluorescent myofibril, which was allowed to shorten for 20% of the myofibril length and then kept in an isometric condition to prevent overshortening and to allow a direct demonstration of the effect of shortening on the nucleotide displacement rate. The shortening regime was imposed 100 ms after the flash to release ATP and fully activate contraction. The triggering of the frame grabber board in the computer was adjusted to start capturing the image at the beginning of the myofibril shortening. A logarithmic plot of fluorescence decay (Fig. 8 *B*) shows that the rate of nucleotide displacement during the shortening phase is clearly different from that during the isometric phase starting from the termination of ramp shortening. The rate constant for nucleotide displacement during the shortening phase was calculated to be 0.4 s^{-1}. A similar value was obtained by an exponential fit to the untransformed data, using the final intensity value as an end point.

To check the effect of movement artifacts on the analysis of fluorescence intensity, a measurement was done for a

myofibril that was allowed to shorten at 10 μM Cy3-EDA-ATP in the presence of Ca^{2+}, but without flash photolysis of caged ATP. The measured fluorescence intensities showed little change during shortening. This indicates that the analytical procedure used caused no artifact due to the myofibril shortening.

In Fig. 9, the displacement rate constant for myofibrils incubated with Cy3-EDA-ATP is plotted against the velocity of myofibril shortening. The rate constant increased from 0.3 s^{-1} to 0.7 s^{-1} as the shortening velocity was increased from zero to 0.2 myofibril length/s, and then decreased with further shortening velocity. The maximum shortening velocity of the myofibril under the solution conditions used was estimated to be ~0.4 myofibril length/s by the observation that myofibril became slack when the imposed shortening velocity exceeded 0.4 myofibril length/s.

DISCUSSION

To monitor the ATP turnover rate of contracting myofibril, we have followed the kinetics of nucleotide exchange (Ferenczi et al., 1989; Sowerby et al., 1993; Myburgh et al., 1995; Conibear and Bagshaw, 1996). Turnover rates were measured by rapidly introducing ATP, by flash photolysis, to displace fluorescent nucleotides prebound to cross-bridges in the myofibril. Although 3′-(2′)-*O*-(*N*-methyl)anthraniloyl-ATP (mant-ATP) is a good fluorescent probe for the actomyosin kinetics in solution (Hiratsuka, 1983; Cremo et al., 1990; Woodward et al., 1991), it shows considerable photobleaching and poor contrast under the fluorescence microscope (Bagshaw et al., 1992). Furthermore, its excitation spectrum overlaps that for caged ATP photolysis. For this reason we turned to EDA-ATP-based analogs containing fluorophores that fluoresce in the visible region (Bagshaw, 1997).

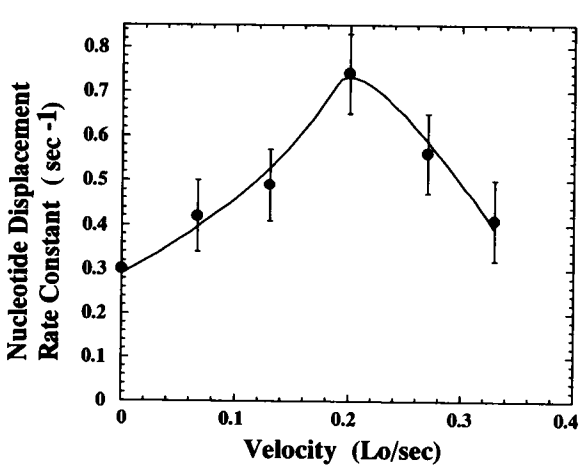

FIGURE 9 Relation between the observed Cy3-EDA-nucleotide displacement rate constant and the velocity of shortening of the myofibril measured simultaneously. The myofibril preparations were bathed in activating solution and induced to shorten as described in Fig. 8. The data represent the average and standard deviation obtained from different myofibril preparations (n = 5). The curve was drawn by eye.

Detection of bound fluorescent nucleotides

Isolated myosin thick filaments are readily visualized with an optical microscope in the presence of low concentrations (<0.1 μM) of fluorescent nucleotide substrates because of the local high concentration of fluorophores bound to the myosin active sites during the steady-state turnover reaction (Sowerby et al., 1993). Preliminary studies with myofibrils using fluorescein and rhodamine derivatives of EDA-ATP demonstrated, as expected, that the A-band was selectively stained (Chaen et al., 1996). However, the study of myofibrils presents several difficulties over that of isolated thick filaments. Actin activation of the ATPase results in potentially faster kinetics of displacement. To resolve processes using conventional video rate acquisition, we carried out measurements at a reduced temperature (8°C). Also as a consequence of actin activation of the ATPase, the K_m for nucleotides would increase, leading to a lower fraction of the myosin sites being occupied at a fixed nucleotide concentration. Increasing the fluorescent nucleotide concentration to counteract this would not lead to improved image contrast because the background signal from the free nucleotide would also increase. A real gain in image contrast can be achieved by using an optical method with enhanced z resolution and by selection of a fluorescent ATP analog that shows an enhancement in emission intensity on binding to myosin (e.g., Cy3-EDA-ATP) rather than a quench, as is observed with fluorescein and rhodamine EDA-ATP derivatives (Conibear et al., 1996).

Although total internal reflectance fluorescence microscopy provides an excellent means of reducing background signal from the bulk fluorophore (Funatsu et al., 1995; Conibear et al., 1995; Conibear and Bagshaw, 1996; Oiwa et al., 1996), the requirement to study molecules within the 150-nm evanescent field at the glass/water interface renders it less versatile for monitoring myofibrils. When a myofibril is attached to glass needles to control or monitor its length and tension, the preparation must be held several microns away from the surface. For this reason we used rapid scanning confocal microscopy to reduce the background signal from the free fluorophore. By this means fluorescence from the A-bands of a myofibril was readily observed against a background of 10 μM Cy3-EDA-ATP. Under optimal conditions, the reduced fluorescence from the M-line region of a myofibril is resolvable (Fig. 2 *A*).

In principle, one might expect to see preferential fluorescence staining of the nonoverlap region of the A-band at intermediate sarcomere lengths, but we have not seen this reproducibly. The K_m values for both the actomyosin and myosin ATPase are less than 10 μM Cy3-EDA-ATP (Fig. 4), and thus heads throughout the sarcomere should be predominantly occupied at this concentration. At lower [Cy3-EDA-ATP], where the difference in K_m values between actomyosin and myosin should be more apparent, there is a greater likelihood of Cy3-EDA-ADP build-up. Moreover, at the shorter sarcomere lengths routinely used (2.5 μm), the 0.15-μm bare zone would tend to dominate

the potentially stronger staining of the myosin heads in the 0.15-μm nonoverlap region either side of it, giving an overall lower intensity at the M-line (Fig. 2 *A*).

Cy3-EDA-ATP as a substrate for myofibril contraction

Cy3-EDA-ATP and other 2′(3′)ribose-modified analogs are reasonable substrates for the myosin and actomyosin ATPase (Sowerby et al., 1993; Saito et al., 1995; Oiwa et al., 1996; Conibear et al., 1996; Bagshaw, 1997). Where measured, the kinetic parameters of the myosin and actomyosin ATPase with Cy3-EDA-ATP, in solution, are within a factor of 2–4 of those of ATP (Eccleston et al., 1996; Conibear et al., 1996). These results are consistent with the finding that the 2′- and 3′-ribose hydroxyls of ATP face outward from the nucleotide pocket in the myosin head structure and are thus free for derivatization (Fisher et al., 1995).

Cy3-EDA-ATP and Cy5-EDA-ATP support actin sliding in in vitro motility assays, although the sliding velocities have only been compared with ATP at low nucleotide concentrations (Saito et al., 1995; Oiwa et al., 1996). Here we show 5 μM Cy3-EDA-ATP supported myofibril contraction, and the auxotonic shortening was comparable to that with 5 μM ATP (Fig. 3). However, in these experiments the velocity of contraction is much less than V_{max} because of the resistance from rigor links at low nucleotide concentration. Eccleston et al. (1996) found that the unloaded shortening velocity of skinned rabbit fast twitch fibers with 0.5 mM Cy5-EDA-ATP was reduced to 10% of that with 0.5 mM ATP.

The maximum velocity of myofibril shortening we observed in the presence of Cy3-EDA-ATP and initiated by flash photolysis of caged ATP was 0.4 myofibril lengths/s at 8°C. This is ~4 times slower than might be expected for shortening induced by ATP itself (1.6 lengths/s at 10°C; Cooke et al., 1988). Two factors could contribute to this result. Cross-bridges using Cy3-EDA-ATP as substrate may show slower cycling kinetics (Eccleston et al., 1996), and/or the residual unphotolysed caged ATP may result in inhibition of sliding (Thirwell et al., 1995). To distinguish between these possibilities, myofibril shortening was followed after flash photolysis of 5 mM caged ATP, in the absence of Cy3-EDA-ATP. Under these conditions the maximum velocity, as judged by the onset of slackness, was 1.2 myofibril lengths/s. Thus it appears that Cy3-EDA-ATP slows down the cross-bridge cycling rate by a factor of ~3. From an estimate of the remaining unphotolysed caged ATP concentration of ~4 mM, the sliding velocity after the generation of 1 mM ATP in the myofibril would be inhibited by a factor of less than 2 (Thirwell et al., 1995).

It should be noted that in our experiments, the initial [Cy3-EDA-ATP] is near or above the K_m for the ATPase (Fig. 4) but below the K_m for shortening, and thus the myofibrils initially remain isometric from the combined effects of a few rigor links and attachment to the stiff needles. On flash photolysis, the resultant ~1 mM ATP concomitantly dissociates remaining rigor links, effects analog displacement, and drives contraction. If allowed to shorten, the cross-bridges could utilize both ATP and Cy3-EDA-ATP to cycle during their first turnover. The fact that a slower sliding rate is observed on photolysis in the presence of Cy3-EDA-ATP compared with its absence suggests that slower turnover of Cy3-EDA-ATP limits the sliding of the whole cross-bridge population, reminiscent of the situation with hybrid myosin filaments in in vitro motility assays (Warshaw et al., 1990). On the other hand, if cross-bridges bearing Cy3-EDA-ATP did not actively cycle, but remained in a rigor-like attached state until the products were released, then a lag in the onset of shortening might be apparent. This would be reflected in an initial slackening of the myofibril when imposed to shorten by the piezo-actuator; however, this was not observed (Fig. 8).

Displacement rate as a measure of myofibril ATPase

At long sarcomere lengths (>3.2 μm) and low [Ca^{2+}], the observed displacement rate constants for Cy3-EDA-ATP and Cy3-EDA-ADP of 0.03 s^{-1} and 0.42 s^{-1}, respectively, at 8°C are in line with those expected for for the myosin ATPase alone (cf. 0.06 s^{-1} and 0.77 s^{-1}, respectively, for the corresponding rhodamine analogs with synthetic myosin filaments at 20°C; Conibear and Bagshaw, 1996). At short sarcomere lengths (2.5 μm), in the presence of Ca^{2+}, the observed rate constants with myofibrils were an order of magnitude faster, indicative of actin activation. In the absence of Ca^{2+}, the rate constants were sixfold lower, but it is likely that the myofibril preparation remains partially activated because the initial nucleotide concentration is low, and hence the regulatory system is overridden by the formation of rigor links (Bremel and Weber, 1972).

Houadjeto et al. (1992) compared the ATPase rates of unloaded myofibrils, cross-linked acto-S1, and S1 alone by transient state methods at 4°C. They concluded that the initial ATP binding and cleavage steps were similar and rapid for all preparations, but in the presence of actin, the rate-limiting product release step was activated from 0.02 s^{-1} to 2 s^{-1}. Thus, for all preparations at low temperatures, the predominant steady-state complex contains a cleaved nucleotide product, although at 20°C the hydrolysis step becomes rate limiting for cross-linked actoS1 (Herrmann et al., 1994).

Importantly, they also found that the release of ATP from the active site without hydrolysis (k_{-2} in their scheme) was less than the turnover rate for all preparations. Thus, in our displacement experiments, it is likely that the observed rate constants for fluorescent ATP analogs reflect the turnover rates alone, rather than having a significant contribution from the back-dissociation rate to give free nucleotide triphosphate. However, there is a possibility that some nu-

cleotide may reversibly bind to secondary nonhydrolytic sites (Houadjeto et al., 1992), which could contribute to the observed displacement reaction.

Taken in conjunction with the above, the difference in myofibril fluorescence intensity and the rate constants for displacement for Cy3-EDA-ATP and Cy3-EDA-ADP argue that the predominant state of the former in the myofibril is M · Cy3-EDA-ADP · P_i or A · M · Cy3-EDA-ADP · P_i (see below), although M · Cy3-EDA-ADP or A · M · Cy3-EDA-ADP may contribute at low [Cy3-EDA-ATP] because of local exhaustion of substrate and product build-up.

Effect of mechanical constraints on nucleotide displacement rate

Previous experiments investigating the effect of load on myofibril ATPase activity have exploited analysis using single turnover conditions (where excess rigor links prevent shortening; Sleep, 1981) or limited chemical cross-linking to maintain the isometric state (Glyn and Sleep, 1985; Herrmann et al., 1994). In the case of unloaded shortening, it was found to be imperative to examine the ATPase kinetics within the first seconds of the reaction before the myofibrils undergo supercontraction (Houadjeto et al., 1992). From interpolation of the data obtained by Herrmann et al. (1994) at 4°C and 10°C, the overall ATPase activities of cross-linked (isometric) and unloaded myofibrils at 8°C are 1.0 and 2.5 s^{-1}, respectively. These values are three- to sixfold higher than those obtained by displacement of Cy3-EDA-ATP (Fig. 9), most likely because the analog is a poorer substrate. Nevertheless, the Cy3-EDA-ATPase appears to be well coupled to the cross-bridge cycle because it slows down the shortening velocity by a comparable amount. Although the mechanochemistry after flash photolysis is complicated by the involvement of two substrates, ATP and Cy3-EDA-ATP, the observed fluorescent signal and mechanics appear to report on the cross-bridge cycle involving Cy3-EDA-ATP. If sliding were driven solely by ATP and those cross-bridges bearing Cy3-EDA-nucleotides simply responded passively, it is unlikely the rate constant for Cy3-EDA nucleotide displacement would show an initial increase with increasing shortening velocities. Thus the biphasic relationship between the observed displacement rate and sliding velocity (Fig. 9) would appear to reflect the Fenn effect observed in intact muscle with its natural substrate (Kushmerick and Davies, 1969; Rall et al., 1976; Homsher et al., 1981).

The data of Fig. 9 also allow a calculation of the mechanochemical coupling properties during unloaded shortening. A sliding velocity of 0.33 myofibril lengths/s corresponds to 0.4 μm/s/half-sarcomere. The corresponding Cy3-EDA-ATP turnover rate constant of 0.4 s^{-1} indicates that, on average, each cross-bridge travels 1 μm for each Cy3-EDA-ATP molecule turned over. Thus, if the cross-bridge power stroke is on the order of 10 nm (Ford et al., 1977; Yamada et al., 1993) and there is 1:1 coupling between the mechanical and biochemical cycles, the majority (99%) of the cross-bridges must remain detached (predominantly in the M · Cy3-EDA-ADP · P_i state) or fail to go through complete turnover cycles during unloaded shortening. If this assumption is correct, then attached states that drive contraction must turnover at $\geq 40\ s^{-1}$. This conclusion is in accord with previous calculations with ATP as substrate (Bagshaw, 1993), which require rapid transitions between attached states as a consequence of the very low duty ratio. By analogy with ADP (Siemankowski et al., 1985), it is possible that the rate of Cy3-EDA-ADP dissociation from A · M · Cy3-EDA-ADP limits the maximum velocity of shortening.

The ability to control the length of a single myofibril and measure its velocity of shortening and tension development by using glass microneedles offers much scope for analysis of its mechanical properties beyond that obtainable with chemically fixed or untethered myofibrils. Here we demonstrate the ability of fluorescence detection to follow events of the ATPase cycle simultaneously with mechanical measurements. In principle, these measurements could be extended to investigate the effects of rapid mechanical perturbations on the chemical states of the cross-bridge (cf. Friedman and Goldman, 1996).

This work was supported by a grant from the Naito Foundation (SC); a Grant-in-Aid for Scientific Research from the Ministry of Education, Science and Culture of Japan, no. 08740655 (IS); and the Uehara Memorial Foundation (HS). CRB was supported by a fellowship from the Japanese Society for the Promotion of Science and The Wellcome Trust, U.K.

REFERENCES

Anazawa, T., K. Yasuda, and S. Ishiwata. 1992. Spontaneous oscillation of tension and sarcomere length in skeletal myofibrils. Microscopic measurement and analysis. *Biophys. J.* 61:1099–1108.

Bagshaw, C. R. 1993. Muscle Contraction, 2nd Ed. Chapman and Hall, London.

Bagshaw, C. R. 1997. Use of fluorescent nucleotides. *In* Current Methods in Muscle Physiology: Advantages, Problems and Limitations. H. Sugi, editor. Oxford University Press, Oxford. In press.

Bagshaw, C. R., M. Matuska, and J. A. Spudich. 1992. Measurement of ATP turnover by single, immobilized myosin filaments. *J. Muscle Res. Cell Motil.* 13:266–267.

Bartoo, M. L., V. I. Popov, L. A. Fearn, and G. H. Pollack. 1993. Active tension generation in isolated skeletal myofibrils. *J. Muscle Res. Cell Motil.* 14:498–510.

Bremel, R. D., and A. Weber. 1972. Cooperation with actin filament in vertebrate skeletal muscle. *Nature New Biol.* 238:97–101.

Chaen, S., I. Shirakawa, I., C. R. Bagshaw, and H. Sugi. 1996. Measurement of ATP turnover in single contracting myofibrils using a fluorescent ATP analogue. *J. Muscle Res. Cell Motil.* 17:280. (Abstr.)

Colomo, F., N. Piroddi, C. Poggesi, and C. Tesi. 1995. Myofibrillar contribution to passive tension in striated muscle. *Biophys. J.* 68:344S. (Abstr.)

Conibear, P. B., and C. R. Bagshaw. 1996. Measurement of nucleotide exchange kinetics with isolated synthetic myosin filaments using flash photolysis. *FEBS Lett.* 380:13–16.

Conibear, P. B., D. S. Jeffreys, C. K. Seehra, R. J. Eaton, and C. R. Bagshaw. 1996. Kinetic and spectroscopic characterization of fluorescent ribose-modified ATP analogs upon interaction with skeletal muscle myosin subfragment 1. *Biochemistry.* 35:2299–2308.

Conibear, P. B., C. K. Seehra, C. R. Bagshaw, and D. Gingell. 1995. Observation of ATP turnover during *in vitro* motility assays. *Biochem. Soc. Trans. (Lond.).* 23:400S. (Abstr.)

Cooke, R. 1986. The mechanism of muscle contraction. *CRC Crit. Rev. Biochem.* 21:53–118.

Cooke, R., and W. Bialek. 1979. Contraction of glycerinated muscle fibers as a function of MgATP concentration. *Biophys. J.* 28:241–258.

Cooke, R., K. Franks, G. B. Luciani, and E. Pate. 1988. The inhibition of rabbit skeletal muscle contraction by hydrogen ions and phosphate. *J. Physiol. (Lond.).* 398:77–97.

Cooke, R., H. White, and E. Pate. 1994. A model of the release of myosin heads from actin in rapidly contracting muscle fibers. *Biophys. J.* 66: 778–788.

Cremo, C. R., J. M. Neuron, and R. G. Yount. 1990. Interaction of myosin subfragment 1 with fluorescent ribose-modified nucleotides: a comparison of vanadate trapping and SH1-SH2 cross-linking. *Biochemistry.* 29:3309–3319.

Eccleston, J. F., K. Oiwa, M. A. Ferenczi, M. Anson, J. E. T. Corrie, A. Yamada, H. Nakayama, and D. R. Trentham. 1996. Ribose-linked sulfoindocyanine conjugates of ATP: Cy3-EDA-ATP and Cy5-EDA-ATP. *Biophys. J.* 70:A159.

Fenn, W. O. 1923. A quantitative comparison between the energy liberated and the work performed by the isolated sartorius muscle of the frog. *J. Physiol. (Lond.).* 58:175–203.

Fenn, W. O. 1924. The relation between the work performed and the energy liberated in muscular contraction. *J. Physiol. (Lond.).* 58: 373–395.

Ferenczi, M. A., S. K. A. Woodward, and J. F. Eccleston. 1989. The rate of Mant-ADP release from cross-bridges of single skeletal muscle fibers. *Biophys. J.* 55:441a.

Fisher, A. J., C. A. Smith, J. Thoden, R. Smith, K. Sutoh, H. M. Holden, and I. Rayment. 1995. Structural studies of myosin: nucleotide complexes: a revised model for the molecular basis of muscle contraction. *Biophys. J.* 68:19s–28s.

Ford, L. E., A. F. Huxley, and R. M. Simmons. 1977. Tension responses to sudden length changes in stimulated frog muscle fibres near slack length. *J. Physiol. (Lond.).* 269:441–515.

Friedman, A. L., and Y. E. Goldman. 1996. Mechanical characterization of skeletal muscle myofibrils. *Biophys. J.* 71:2774–2785.

Funatsu, T., Y. Harada, M. Tokunaga, K. Saito, and T. Yanagida. 1995. Imaging of single fluorescent molecules and individual ATP turnovers by single myosin molecules in aqueous solution. *Nature.* 374:555–559.

Glyn, H., and J. Sleep. 1985. Dependence of adenosine triphosphatase activity of rabbit psoas muscle fibers and myofibrils on substrate concentration. *J. Physiol. (Lond.).* 365:259–276.

Goldman, Y. E. 1987. Kinetics of the actomyosin ATPase in muscle fibers. *Annu. Rev. Physiol.* 49:637–654.

Herrmann, C., C. Lionne, F. Travers, and T. Barman. 1994. Correlation of actoS1, myofibrillar, and muscle fiber ATPases. *Biochemistry.* 33: 4148–4154.

Herrmann, C., J. Sleep, P. Chaussepied, F. Travers, and T. Barman. 1993. A structural and kinetic study on myofibrils prevented from shortening by chemical cross-linking. *Biochemistry.* 32:7255–7263.

Hibberd, M. G., and D. R. Trentham. 1986. Relationship between chemical and mechanical events during muscular contraction. *Annu. Rev. Biophys. Biophys. Chem.* 15:119–161.

Hill, A. V. 1964. The effect of load on the heat of shortening of muscle. *Proc. R. Soc. Lond. B Biol. Sci.* 159:297–318.

Hiratsuka, T. 1983. New ribose-modified fluorescent analogs of adenine and guanine nucleotides available as substrates for various enzymes. *Biochem. Biophys. Acta.* 742:496–508.

Homsher, E. 1987. Muscle enthalpy production and its relationship to actomyosin ATPase. *Annu. Rev. Physiol.* 49:673–690.

Homsher, E., M. Irving, and A. Wallner. 1981. High-energy phosphate metabolism and energy liberation associated with rapid shortening in frog skeletal muscle. *J. Physiol. (Lond.).* 321:423–436.

Houadjeto, M., F. Travers, and T. Barman. 1992. Ca^{2+}-activated myofibrillar ATPase: transient kinetics and the titration of its active sites. *Biochemistry.* 31:1564–1569.

Huxley, A. F. 1957. Muscle structure and theories of contraction. *Prog. Biophys. Biophys. Chem.* 7:255–318.

Huxley, A. F. 1973. A note suggesting that the cross-bridge attachment during muscle contraction may take place in two stages. *Proc. R. Soc. Lond. B.* 183:83–86.

Kushmerick, M. J., and R. E. Davies. 1969. The chemical energetics of muscle contraction. II. The chemistry, efficiency and power of maximally working sartorius muscles. *Proc. R. Soc. Lond. B Biol. Sci.* 174:315–353.

Lionne, C., M. Brune, M. R. Webb, F. Travers, and T. Barman. 1995. Time resolved measurements show that phosphate release is the rate limiting step on myofibrillar ATPases. *FEBS Lett.* 364:59–62.

Lionne, C., F. Travers, and T. Barman. 1996. Mechanochemical coupling in muscle: attempts to measure simultaneously shortening and ATPase rates in myofibrils. *Biophys. J.* 70:887–895.

Ma, Y.-Z., and E. W. Taylor. 1994. Kinetic mechanism of myofibril ATPase. *Biophys. J.* 66:1542–1553.

Mujumdar, R. B., L. A. Ernst, S. R. Mujumdar, C. J. Lewis, and A. S. Waggoner. 1993. Cyanine dye labeling reagent: sulphoindocyanine succinimidyl esters. *Bioconj. Chem.* 4:105–111.

Myburgh, K. H., K. Franks-Siba, and R. Cooke. 1995. Nucleotide turnover rate measured in fully relaxed rabbit skeletal muscle myofibrils. *J. Gen. Physiol.* 106:957–973.

Ohno, T., and T. Kodama. 1991. Kinetics of adenosine triphosphate hydrolysis by shortening myofibrils from rabbit psoas muscle. *J. Physiol. (Lond.).* 441:685–702.

Oiwa, K., M. Anson, A. Yamada, J. F. Eccleston, J. E. T. Corrie, M. A. Ferenczi, D. R. Trentham, and H. Nakayama. 1996. Microscopic observations of Cy3-EDA-ATP and Cy5-EDA-ATP binding to myosin filaments *in vitro*. *Biophys. J.* 70:A159.

Rall, J. A., E. Homsher, A. Wallner, and W. F. H. M. Mommaerts. 1976. A temporal dissociation of energy liberation and high energy phosphate splitting during shortening in frog skeletal muscles. *J. Gen. Physiol.* 68:13–27.

Saito, K., M. Tokunaga, H. Yokota, and T. Yanagida. 1995. ATPase reaction during sliding of actin filaments. *Biophysics (Jpn. Biophys. Soc.).* 35:S208. (Abstr.)

Siemankowski, R. F., M. O. Wiseman, and H. D. White. 1995. ADP dissociation from actomyosin subfragment1 is sufficiently slow to limit the unloaded shortening velocity in vertebrate muscle. *Proc. Natl. Acad. Sci. USA.* 82:628–662.

Sleep, J. A. 1981. Single turnovers of adenosine 5′-triphosphate by myofibrils and actomyosin subfragment 1. *Biochemistry.* 20:5043–5051.

Sowerby, A. J., C. K. Seehra, M. Lee, and C. R. Bagshaw. 1993. Turnover of fluorescent nucleotide triphosphates by isolated immobilized myosin filaments. Transient kinetics on the zeptomole scale. *J. Mol. Biol.* 243:114–123.

Sugi, H. 1992. Molecular mechanism of actin-myosin interaction in muscle contraction. *In* Muscle Contraction and Cell Motility: Molecular and Cellular Aspects. H. Sugi, editor. Springer-Verlag, Berlin and Heidelberg. 132–171.

Sugi, H. 1997. Muscle mechanics I and II. *In* Current Methods in Muscle Physiology: Advantages, Problems and Limitations. H. Sugi, editor. Oxford University Press, Oxford. In press.

Taylor, E. W. 1979. Mechanism of actomyosin ATPase and the problem of muscle contraction. *CRC Crit. Rev. Biochem.* 6:103–164.

Thirwell, H., J. A. Sleep, and M. A. Ferenczi. 1995. Inhibition of unloaded shortening velocity in permeabilized muscle fibres by caged ATP compounds. *J. Muscle Res. Cell Motil.* 16:131–137.

Warshaw, D. M., J. M. Desrosiers, S. S. Work, and K. M. Trybus. 1990. Smooth muscle myosin cross-bridge interactions modulate actin filament sliding *in vitro*. *J. Cell. Biol.* 111:453–463.

Woodward, S. K. A., J. F. Eccleston, and M. A. Geeves. 1991. Kinetics of the interaction of 2′(3′)-*O*-(*N*-methylanthraniloyl)-ATP with myosin subfragment 1 and actomyosin subfragment 1: characterization of two actoS1ADP complexes. *Biochemistry.* 30:422–430.

Yamada, T., O. Abe, T. Kobayashi, and H. Sugi. 1993. Myofilament sliding per ATP molecule in rabbit skeletal fibres using laser flash photolysis of caged ATP. *J. Physiol. (Lond.).* 466:229–243.